

Online HPLC Analysis of Buchwald-Hartwig Aminations from Within an Inert Environment

Thomas C. Malig, Lars P. E. Yunker, Sebastian Steiner, Jason E. Hein*

†Department of Chemistry, University of British Columbia, 2036 Main Mall, Vancouver, British Columbia V6T 1Z1, Canada

ABSTRACT: Obtaining data dense reaction profiles for reactions performed under an inert atmosphere remains a significant challenge obfuscating mechanistic analysis. To this end, we have developed a reaction monitoring platform capable of automated sampling and online HPLC analysis to generate temporal profiles for reactions performed from within a glovebox. The device allows for facile reaction progress analysis to aid in mechanistic studies of air-sensitive chemical transformations. The platform has demonstrated high reproducibility regarding sample mixing, dilution, delivery, and analysis. We employed the sampling platform to acquire temporal profiles for a series of Buchwald-Hartwig aminations. Parallel coupling reactions using iodobenzene and bromobenzene both exhibit complex kinetics. A competition reaction including both aryl halides demonstrated high selectivity for iodobenzene indicative of catalyst monopoly. The temporal profile for the difunctionalized substrate 1,4-iodobromobenzene was unexpected based *a priori* and is indicative of a distinct underlying mechanism. We attribute this unanticipated reactivity to intramolecular catalysts transfer through the π system as seen in “living” polymerization transfer catalyst systems. This automated sampling platform has greatly increased mechanistic understanding by performing only a small subset of experiments.

INTRODUCTION

The combination of automated sampling with online, chromatographic analysis represents an optimal method for gathering temporal reaction data with minimal analyst intervention. The resolving ability of HPLC allows for the quantification of starting materials, intermediates, products, and byproducts from complex mixtures, making it an invaluable tool for reaction profiling to facilitate mechanistic analysis. Specifically, employing online HPLC for reaction monitoring facilitates the construction of accurate concentration vs time profiles of structurally similar components without a chemometric model. Online HPLC offers unmatched mechanistic information in a small subset of experiments not possible with other operando techniques such as in situ IR or calorimetry.

Recently, we reported a reaction monitoring platform capable of autonomous aliquoting, sample delivery, and online analysis using HPLC to aid us in mechanistic investigations.^{1,2} The ubiquity of useful, air sensitive transformations coupled with the difficulty of gathering temporal data without compromising their inert atmosphere prompted us to modify our sampling device. We envisioned that we could expand the reaction monitoring scope of the system to allow for profiling of air-sensitive reactions. Herein, we present our modified reaction monitoring platform (Figure 1), which is capable of automated sampling and online HPLC analysis from reactions performed under an inert atmosphere (inside a glovebox).

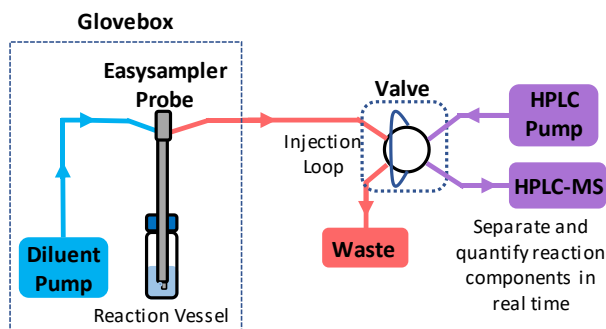
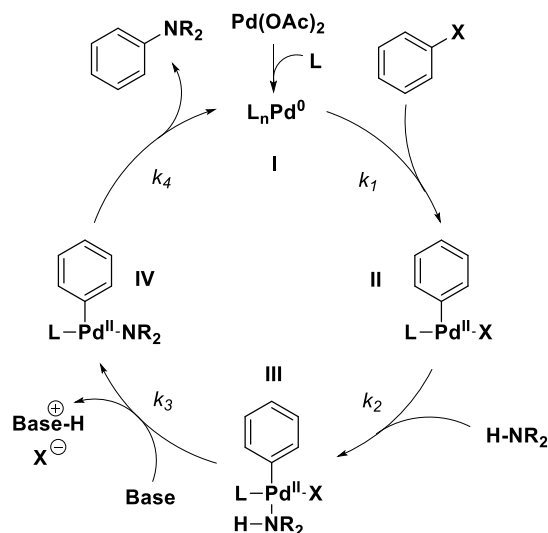


Figure 1: Cartoon schematic of automated the reaction monitoring platform used to gather time-course data from reactions performed within a glovebox.

Once assembled we first probed the system's ability to sample, dilute, mix, and analyze aliquots reproducibly collected within an inert environment. We then employed the platform to monitor a series of Buchwald-Hartwig amination reactions, a catalytic transformation for forming C-N bonds.³ This extremely useful transformation has become a fundamental tool in organic synthesis for the formation of C(sp²)-N bonds.³⁻⁶ Since the seminal reports by Buchwald⁷ and Hartwig⁸, the Buchwald-Hartwig

amination has seen widespread use in the synthesis of pharmaceuticals,^{9–13} natural products,^{14,15} organic materials,¹⁶ and agrochemicals.¹⁷

A simplified catalytic cycle for a Buchwald-Hartwig amination using Pd(OAc)₂ as a precatalyst is depicted in Scheme 1. First, activation of Pd(OAc)₂ via a reducing agent forms the catalytically active Pd(0) species I. The cross-coupling catalytic cycle proceeds through four key intermediates (I–IV). Phosphine ligated palladium I undergoes oxidative addition with the aryl halide to generate complex II. Coordination of the amine forms *N*-bound palladium complex III, which reacts with base to form the amido complex IV. Reductive elimination of IV forms the key C–N bond, simultaneously liberating both the cross-coupled product and the Pd(0) species I, where it can reenter the catalytic cycle. This simplified model does not account for effects of off-cycle species or palladium aggregates, each of which can impact the overall reaction rate.^{18,19}



Scheme 1. Generic catalytic cycle for the palladium-catalyzed coupling of iodobenzene with arylamines.

RESULTS AND DISCUSSION

The Reaction Monitoring Platform

The automated reaction monitoring platform uses an Arduino microcontroller to initiate all sampling events. A computer executing a Python script communicates with the microcontroller to sequence events similar to what has been described previously.^{1,20–22} A schematic displaying core components of the device is displayed in Figure 1.

The sampling sequence begins by priming all fluidic lines with diluent (often the reaction solvent). Next, the slurry probe (Easysampler) is actuated to extend the sampling pocket into the reaction vial. After five seconds, the pocket containing reaction solution is retracted into the probe. The sample aliquot is then delivered via a Cavro syringe pump with an adjustable diluent volume and flow rate outside the glovebox via an air-tight union to an injection loop on a nanovalue. The microcontroller then switches the valve position aligning the sample loop between the HPLC pump and column for analysis. The system resets to its initial state and a wash cycle is performed (2.0 mL of diluent) to flush any residual sample from the fluidic lines and injection loop into the waste. This wash cycle also backfills the probe pocket with clean solvent before the next sample is taken. An important consequence of this wash cycle is dilution of the reaction. Every time the sampling probe extends the pocket into the flask the reaction becomes diluted proportional to the volume of the pocket.

Sample Reproducibility

Before we began acquiring progress curves of air sensitive reactions, we probed the sampling reproducibility by sampling a vial of toluene within the glovebox and measuring the HPLC response on the benchtop. Since the sampling sequence begins with a dilution proportional to the volume of the sample pocket, we would anticipate a negative trend in the diode array detector (DAD) response as a function of the injection number. If observed, this trend would validate the ability of the platform to sample, dilute, and mix aliquots reproducibly, and has the additional benefit of allowing us to calculate the slurry probe pocket volume.

Sampling a vial of toluene from within the glovebox 50 times resulted in a linear trend ($R^2 = 0.99$) with a negative slope (Figure 2a). By using the initial response, slope of the line, and initial volume we were able to calculate the pocket volume of the Easysampler to equal 20.2 μL , which is in excellent agreement with product specifications. This similarity between expected and actual pocket volume demonstrates the ability of the platform to reproducibly collect, mix, dilute, and deliver an aliquot from within the glovebox to an HPLC on the benchtop for real-time analysis.

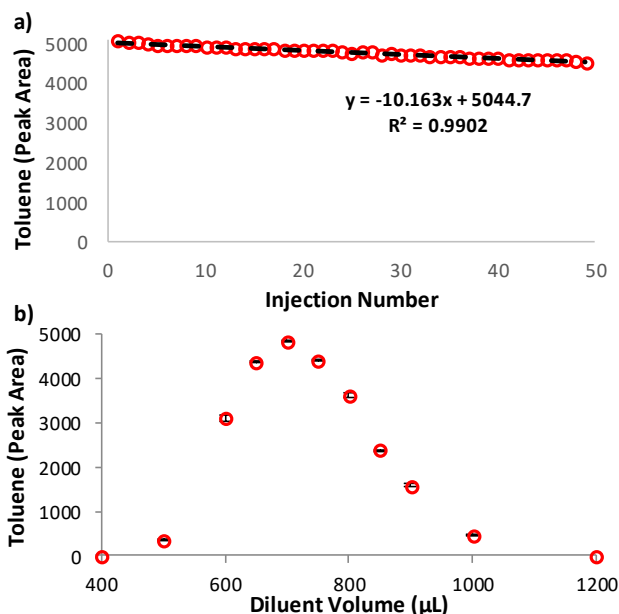
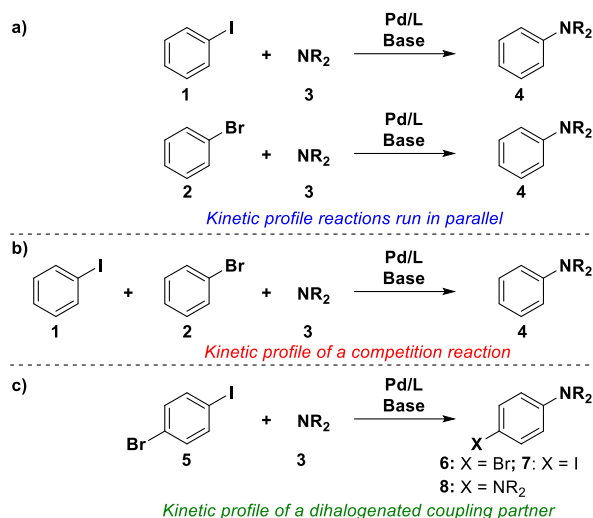


Figure 2: a) Relationship between detector response and sample number when a vial of toluene is sampled 50 times from within a glovebox. b) Relationship between diluent volume and detector response when a vial of toluene is sampled from within a glovebox. Each data point represents the average of a triplicate series. Error bars represent \pm one standard deviation of the series.

Earlier prototypes of our automated sampling platform displayed a unique relationship between diluent volume and detector response.¹ Because of the similarity in design regarding sample mixing and delivery, we would anticipate a similarly shaped trend with this modified platform. By adjusting the diluent volume between 400 – 1200 μL and measuring the response at the detector, we observed a trend shape as anticipated (Figure 2b). A volume in excess of 400 μL (the approximate dead volume between the sample pocket and injection loop) is required to deliver the sample from the reaction vial to the injection loop. Volumes between 400 – 700 μL correspond to a region of growing signal response until a maximum response was observed with a volume of 700 μL . For diluent volumes >700 μL we observe a downward trending response until no signal is received at the detector (1200 μL), indicating that the entire sample has been flushed into the waste. The DAD response for each diluent volume was collected in triplicate and the standard error was plotted (Y error bars). We were pleased to observe low relative standard deviations (often $< 1\%$) further evidencing the high degree of reproducibility the sampling platform can achieve. Therefore, we have demonstrated that by adjusting the diluent volume we can perform on-the-fly, reproducible dilutions. This dynamic dilution data can be utilized to optimize signal response at the detector depending on solution concentration. Concentrated reactions can be diluted more by using volumes either before or after the apex volume (700 μL), whereas reactions of low concentration can receive maximum signal by using the apex delivery volume (700 μL).

Monitoring Buchwald-Hartwig Aminations

The series of Buchwald-Hartwig aminations we chose to monitor is outlined in Scheme 2. We sought to answer the following fundamental questions. First, how does varying the aryl halide between iodobenzene (**1**) and bromobenzene (**2**) effect the reaction profiles of the starting materials and products (Scheme 2a)? Next, what would the reaction progress of a competition reaction using both iodobenzene and bromobenzene look like (Scheme 2b)? And finally, what temporal profile would we observe for the cascade reaction using the dihalogenated substrate 1-bromo-4-iodobenzene (**5**) (Scheme 2c)? The structural similarities between compounds **1-8** complicate quantitation and profiling by spectroscopic methods because of expected signal overlap. By employing HPLC as an analytical tool, starting materials, products, and intermediates can be quantified over the reactions entirety to provide a more detailed mechanistic picture.



Scheme 2. Buchwald-Hartwig amination reactions to be investigated utilizing the automated reaction monitoring platform. Temporal profiles generated from reactions performed under an inert atmosphere (inside a glovebox). R = *p*-methoxyphenyl

COPASI Modeling

Before monitoring the reactions described in Scheme 2, we created models using COPASI software for each case. These models provide a useful starting point to approximate trends based off assumptions made from literature precedence. Previous studies comparing oxidative additions of iodo- and bromobenzene to Pd(0) complexes occur with different kinetic behaviours. Aryl iodides undergo oxidative addition more rapidly than aryl bromides, indicating that the halide identity affects the reaction rate.^{23–26} Additionally, Buchwald demonstrated that reductive elimination of electron rich amines such as **3** is not a kinetically difficult step in certain Pd catalyzed C-N aminations. This observation further supports a paradigm where oxidative addition could be turnover limiting.²⁷ Other mechanistic studies on aminations of aryl bromides revealed conclusively that the secondary amine component does not exhibit positive order kinetics, while a dependence of the rate on [aryl halide] was observed.²⁸ Considering both previous kinetic studies and energy differences between Ph-Br and Ph-I bonds^{29,30}, we will assume that oxidative addition is turnover limiting. Therefore, differences in bond strengths between Ph-I and Ph-Br would manifest in a larger rate of consumption of PhI than PhBr.

For the reactions completed in parallel (Scheme 2a) we assume that the oxidative addition of the aryl halide represents the turnover limiting step to form complex II (Scheme 1). To exemplify these differences in reactivity of the aryl halides, a simplified model in COPASI was constructed (Figure 3a). In this model we assumed that k_1 with iodobenzene is threefold larger than k_1 with bromobenzene. The trends in Figure 3a show first order decay of iodobenzene (**1**) and bromobenzene (**2**) with the rate of consumption of **1** being greater. Therefore, we anticipate that the kinetic profile for the parallel reactions described in Scheme 2a would resemble the temporal profile visualized in Figure 4a.

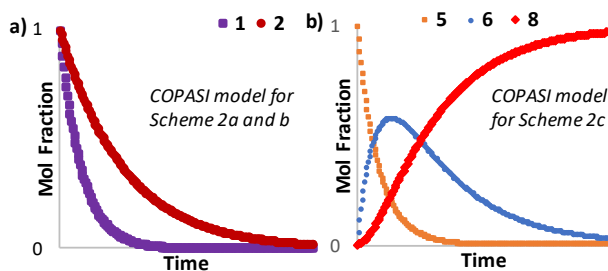


Figure 3: COPASI modelling for the reaction network outlined in Scheme 2. a) Predicted reaction progress curves for competition / parallel aminations (Scheme 2a and b). b) Predicted reaction progress curves for the cascade reaction using 1-bromo-4-iodobenzene (Scheme 2c).

For the competition reaction using two aryl halides (Scheme 2b), we would anticipate simultaneous consumption of PhI and PhBr. Similarly, differences in lability of Ph-I and Ph-Br would result in a larger rate of consumption of iodobenzene vs bromobenzene. Therefore, we expect minimal differences in the kinetic profiles for the parallel and competition reactions described in Scheme 2a and 2b, and that both will resemble the COPASI generated profile displayed in Figure 3a.

The temporal profile for the cascade reaction using the dihalogenated substrate **5** (Scheme 2c) would be an extension of the same hypothesis, where the Ph-I bond engages more readily than Ph-Br leading to a buildup of intermediate **6**. A model was made in COPASI which assumed that coupling would occur exclusively at the C-I position of **6** due to differences in bond strengths of the two halogens (Figure 3b). The additional assumption was made that the rate of oxidative addition for iodobenzene is threefold larger than for bromobenzene. The COPASI model displayed first order decay of **5** as monocoupled intermediate **6** is formed. Eventually **6** hits a maximum concentration as the [**5**] continues to decrease. Next, intermediate **6** enters a

new regime where its rate of consumption exceeds its rate of formation resulting in an inflection point in the [6]. The model predicts a sigmoidal profile for the formation of the dicoupled product 8 as 6 is a necessary precursor.

Parallel reaction data

To demonstrate the ability of our automated sampling device to monitor reactions performed from within a glovebox, we acquired progress curves for a series of Buchwald-Hartwig aminations (Scheme 2). Many developments have been made in optimizing the Buchwald-Hartwig amination to expand the scope and utility of this transformation, but ultimately the selection of the optimal solvent, base, Pd source, and ligand mostly depend on the nature of the substrates.³¹ For our studies we selected the bis(4-methoxyphenyl)amine (3) as our amine coupling partner. We opted to use Pd(OAc)₂ as a precatalyst, as after in situ reduction a highly active Pd catalyst is generated providing superior results to Pd₂(dba)₃, Pd(OAc)₂/PhB(OH)₂ or [(allyl)PdCl]₂ for the arylation of anilines.³² As a ligand we chose the sterically hindered alkyl phosphine P(*t*-Bu)₃ as it is competent for coupling aryl halides and aryl amines.^{33,34} The pyrophoricity and ease of oxidation of P(*t*-Bu)₃ necessitate its usage under an inert atmosphere, providing an excellent test case for our sampling system. Commonly employed bases in the Buchwald-Hartwig amination include NaOtBu,³⁵ LiHMDS,³⁶ and Cs₂CO₃.³⁷ We selected the base/solvent combination of LiHMDS and THF to improve reproducibility, as physical properties such as base particle size can affect the reaction rate in heterogeneous palladium-catalyzed aminations.³⁸ The moisture sensitive nature of LiHMDS further incentivized the use of an inert atmosphere when performing these coupling reactions, thereby additionally validating the use of a glovebox.

We began our reaction monitoring studies using a model system to compare the rates and reaction profiles of C-N coupling with diarylamine bis(4-methoxyphenyl)amine (3) and both iodobenzene (1) and bromobenzene (2). Performing two coupling reactions using identical experimental conditions but with different halide substituents (1 or 2) produced two distinct reaction profiles (Figure 4). Concentrations for 1, 2, 3, and 4 were calculated from external calibration curves created for each component (See SI).

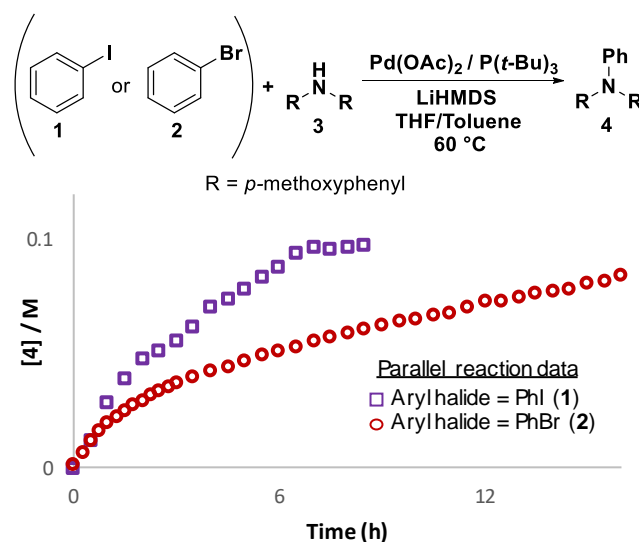


Figure 4: Online HPLC Data for the parallel coupling reactions including aryl halides 1 or 2. Reaction conditions: [1]₀ or [2]₀ = [3]₀ = 0.11 M; [LiHMDS]₀ = 0.165 M; [Pd(OAc)₂]₀ = 2.8 mM; [P(*t*-Bu)₃] = 5.6 mM in THF/toluene (17:1) at 60 °C in a glovebox.

The data in Figure 4 show that neither reaction displays a simple kinetic profile. Interestingly, after the first 30 minutes, the rates for both reactions were comparable. This observation contests our straightforward hypothesis that lability of the C-X bond will dictate the reaction rate. After 3 hours the rate of consumption of bromobenzene decreased until a constant reaction rate was observed, corresponding to 33% conversion of 2. This unchanging rate despite continual reaction progress could indicate a change in the catalyst resting state as a function of turnover for the bromobenzene reaction. Alternatively, the reaction progress when iodobenzene is employed displays a relatively constant reaction rate indicating that the halide identity effects the reaction mechanism. This conclusion is within agreement by rate studies completed by Hartwig, which indicated that the mechanism of oxidative addition differs when iodobenzene and bromobenzene are subjected to identical reaction conditions.²⁴

The non-classical behavior observed in both cases could be a result of catalyst activation/deactivation, formation of aggregates, or a change in the catalyst resting state. Simply performing initial rate measurements would result in the oversimplification of complex kinetic behaviour as observed here. Therefore, the ability of our reaction monitoring platform to observe trends over the entire reaction has unparalleled value for increasing mechanistic understanding, especially in systems that display complex kinetics.

Competition Reaction Data

To further probe the ability of the reaction monitoring platform to profile complex multicomponent reactions, we devised a Buchwald-Hartwig competition reaction using two aryl halides. Competition reactions can be a useful strategy for delineating mechanisms, as they can provide insight to multistep catalytic pathways which cannot be obtained via completing reactions singly.³⁹

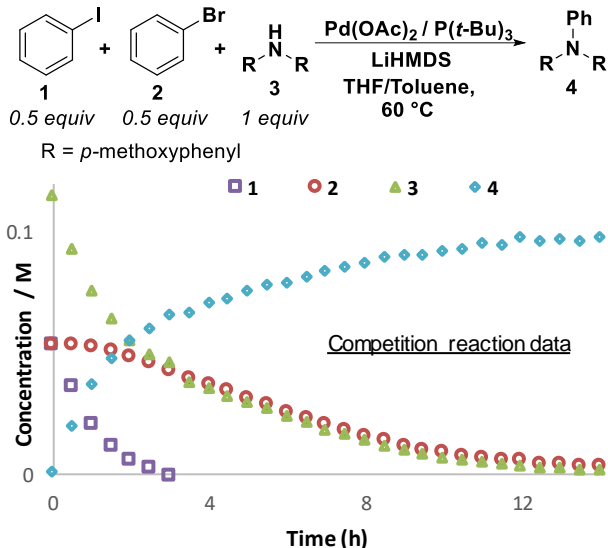
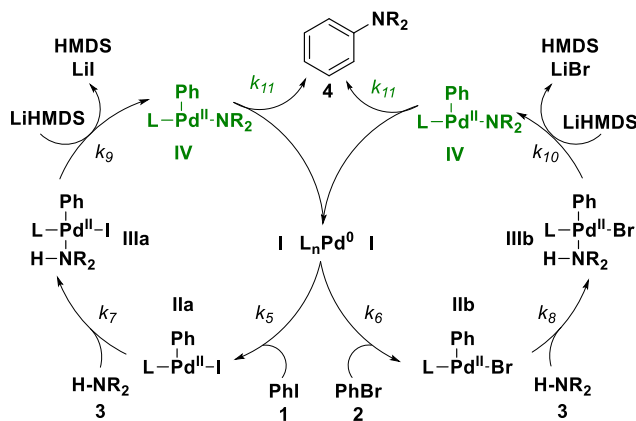


Figure 5: Online HPLC data displaying progress curves for the competition reaction using coupling partners **1** and **2**. Reaction conditions: $[1]_0 = [2]_0 = 0.055 \text{ M}$; $[3]_0 = 0.11 \text{ M}$; $[\text{LiHMDS}]_0 = 0.165 \text{ M}$; $[\text{Pd}(\text{OAc})_2]_0 = 2.8 \text{ mM}$; $[\text{P}(t\text{-Bu})_3] = 5.6 \text{ mM}$ in THF/toluene (17:1) at $60 \text{ }^\circ\text{C}$ in a glovebox.

Both iodobenzene (**1**, 0.5 equiv) and bromobenzene (**2**, 0.5 equiv) were included as coupling partners with arylamine **3** (1 equiv) to form the single triarylamine product **4**. Finding a means to gather time-course data for competition reactions such as this is nontrivial. More routine reaction monitoring techniques such as IR and NMR would likely be incapable of quantifying the reaction species due to signal overlap of structurally similar compounds. Our system, however, is ideally suited for monitoring this multicomponent reaction because it is capable of quantifying **1**, **2**, **3**, **4**, and toluene throughout the entire reactions progress (See SI).

Utilizing the parallel coupling data and COPASI modelling as templates to predict reactivity for the competition reaction, we anticipated simultaneous consumption of both **1** and **2**, with the rate of consumption of **1** being greater (Figure 3a). Instead, we observed a reaction profile with two distinct reactivity regimes (Figure 5). Complete consumption of iodobenzene was observed in under four hours and displayed exponential decay. During this time, the consumption of bromobenzene was minor, indicating high selectivity for coupling **1** over **2** when both are present in similar concentrations. Upon exhaustion of iodobenzene, the rate of consumption of bromobenzene first increases, then decreases until complete consumption was observed after ~14 hours. This sigmoidal profile of **2** was unexpected based off the reactions performed in parallel, and further reinforces the importance of robust time-course data for understanding reaction mechanisms. Often chemical processes are more complex than initially expected and making mechanistic proposals for systems based solely on initial rate or endpoint analysis can lead to faulty understanding. We are confident in the accuracy of the acquire time-course data as we observed a conservation of mass balance throughout the reactions progress. Additionally, the near overlaid trends of **2** and **3** at times >4h exemplify the quantitative accuracy of the platform by accounting for the 1:1 stoichiometry of the reaction.

The observed selectivity for depleting iodobenzene over bromobenzene at the early stages of the reaction is indicative of catalyst monopoly and can be rationalized by either comparing the rates of oxidative addition or the reactivity of downstream intermediates. The competition reaction mechanism can be described as two separate catalytic cycles, one for each aryl halide, and with each beginning at L_nPd^0 (**I**, Scheme 3). Interestingly, both catalytic cycles form the same amido-complex **IV**, so the rate of reductive elimination to form the final product **4** should have negligible effects on the reaction progress.



Scheme 3. Reaction mechanism for the competition reaction using iodobenzene (**1**) and bromobenzene (**2**). R = *p*-methoxyphenyl

Differences in the facileness of the oxidative addition of iodobenzene and bromobenzene could account for the observed catalyst monopoly. If the magnitude of $k_5 \gg k_6$, then oxidative addition complex **IIa** would form preferentially over **IIb**. However, this discrepancy of rate constants between oxidative addition is not supported by the parallel studies, where initial rates for coupling PhBr and PhI were comparable. Alternatively, reactivity differences of later intermediates could account for the observed monopoly. For example, differences in the rate constants k_7 and k_8 to form coordination complexes **IIIa** and **IIIb**, respectively, could manifest as a higher rate of consumption of **IIa** over **IIb**. A final consideration regarding the catalyst monopoly is the possibility that oxidative addition of the C-X bond is reversible. Several examples have been reported indicating that oxidative addition of C-Br is reversible when the bulky ligand P(*t*Bu)₃ is used.⁴⁰⁻⁴² Therefore if formation of **IIb** from **1** and **2** is reversible, and **IIa** is more reactive than **IIb**, the observed monopoly could be a result of a Curtin-Hammett type paradigm. Differences in the stability of oxidative addition complexes **IIa** and **IIb** becomes less relevant, as reactivity of these intermediates is the main driving force for the observed selectivity.

An expanded model in COPASI was created to rationalize the observed catalyst monopoly. In our model, we observed excellent fit for the reaction profiles of all measured species throughout the competition reaction (See SI). Using the model we report that differences in the magnitude of oxidative addition (k_5 vs k_6) accounts for the observed catalyst monopoly, a proposal consistent with previous studies.²⁹

Cascade Reaction Data

To further solidify the capability of the automated sampling platform to generate reaction profiles of complex chemical systems, we chose to monitor an additional C-N coupling reaction using the difunctionalized aryl halide 1-bromo-4-iodobenzene (**5**). Data from the previous parallel and competition reactions would suggest that C-N coupling at the iodo- position of **5** would out-compete coupling at the bromo- position to accumulate a detectable amount of mono-coupled intermediate **6** (Scheme 2c). We would then expect a second regime to predominate involving the coupling of intermediate **6** with an additional molecule of **3** to afford the dicoupled product **8** (Figure 3b).

Combining equimolar amounts of **3** and **5** under coupling conditions instead resulted in another unexpected reaction profile (Figure 6). Strikingly, we observed the dicoupled product **8** on our first collected data point. This result further exemplifies that proposing reaction mechanisms using temporal data of similar catalytic systems is insufficient and can lead to simplified and erroneous understanding. Collecting time course data of each modified system is the only way to truly elucidate mechanistic subtleties. We observed overall zero order decay for the consumption of both starting materials **3** and **5**. The consumption rates of **3** and **5** were 4.4 mM/h and 2.9 mM/h, respectively. This discrepancy between consumption rates can be rationalized mechanistically as **5** reacts only with **3** to form **6**, whereas **3** also reacts with **6** to form **8**.

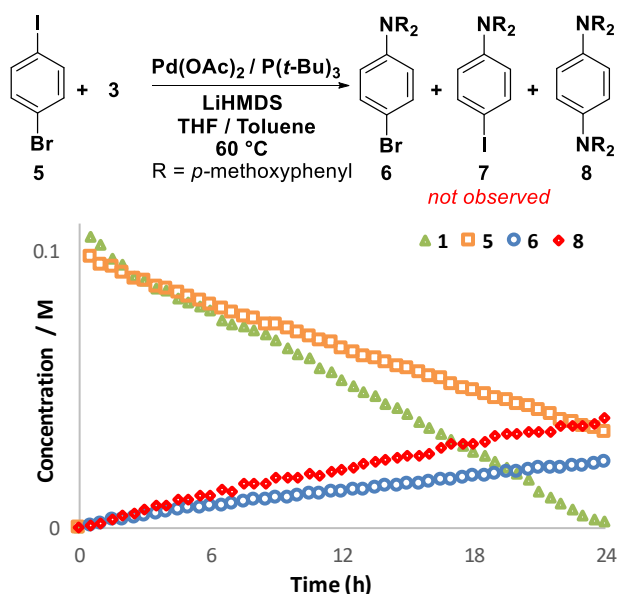


Figure 6: Progress curves when 1-bromo-4-iodobenzene (**5**) is used as the aryl halide coupling partner.

To account for the observed kinetic profile when 1-bromo-4-iodobenzene (**5**) was selected as the halogenated substrate (Figure 6) a linear reaction network was assumed comprising two sequential catalytic cycles. Using COPASI, three models were generated where the magnitudes of k_{12} and k_{13} were adjusted to attempt to match the model with the observed profile. First, $k_{12} = 10k_{13}$ (Figure 7a), then $10k_{12} = k_{13}$ (Figure 7b), and finally $k_{12} = k_{13}$ (Figure 7c).

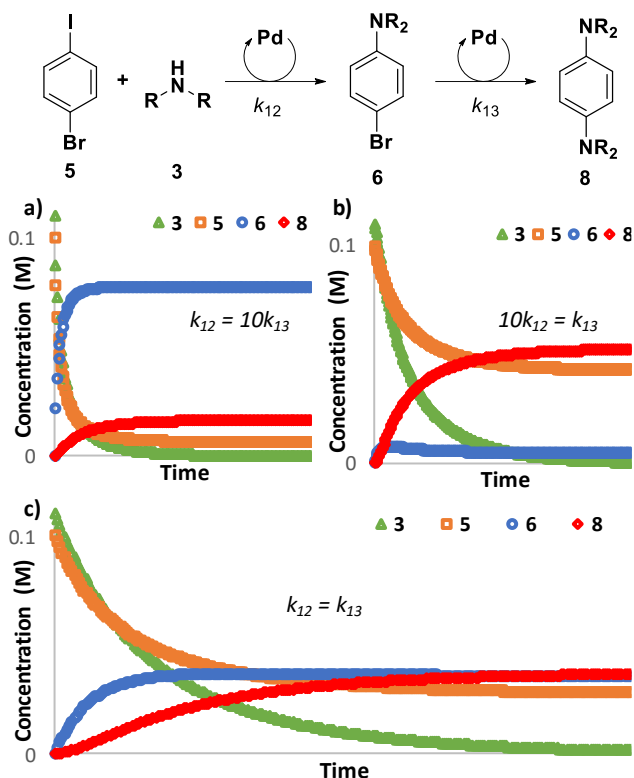
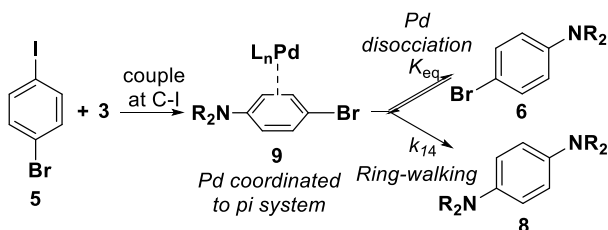


Figure 7. COPASI models for a linear reaction network describing reactivity of **5**. k_{12} and k_{13} values were varied to attempt to match the trends in Figure 6. a) $k_{12} = 10k_{13} = 1 \text{ Ms}^{-1}$; b) $10k_{12} = k_{13} = 1 \text{ Ms}^{-1}$; c) $k_{12} = k_{13} = 0.1 \text{ Ms}^{-1}$

The COPASI models generated in Figure 7, which assumes a linear reaction network, provide a simple but useful approach to delineating the coupling cascade depicted in Figure 6. When the magnitude of the rate constant of the first catalytic cycle (k_{12}) is tenfold larger than that of the second cycle (k_{13}), we would observe **6** as the major product with less than 20% of the dicoupled product **8** being formed (Figure 7a). The large discrepancy of concentrations between **6** and **8** at the end of the reactions progress out this scenario. When the magnitude of the rate constant of the second catalytic cycle (k_{13}) is tenfold larger than that of the first cycle (k_{12}), we observe a change in the selectivity of the major product (Figure 8b). In this scenario, formation of the dicoupled product **8** predominates, while the concentration of intermediate **6** remains low. A maximum **[6]** is observed corresponding to $\sim 10\%$. Finally, when the magnitude of the rate constants for the first and second catalytic cycle are equal ($k_{12} = k_{13}$, Figure 7c), the dicoupled product **8** forms only after an appreciable quantity of **6** has been generated. Interestingly, at the end of the reaction **[6] = [8]**. The nonzero-order profiles predicted in all three of these scenarios, coupled with the product distributions, lead us to believe that this linear model does not accurately account for the observed trends.

To more accurately model the temporal profile observed in Figure 6, we propose an alternate reaction network (Scheme 4). This mechanism invokes π -coordination complex **9**, which is formed after C-N coupling at the iodo-position. We propose intermediate **9** is in equilibrium with **6** and Pd(0).



Scheme 4. Alternate reaction network invoking ring-walking to synthesize **8**.

Invoking **9** allows **8** to be generated directly via a catalyst transfer type mechanism, therefore beginning the second catalytic cycle without liberating **6**. This intramolecular catalyst transfer has been implicated in multiple examples of Pd catalyzed polymerizations of multifunctionalized aryl halides and is commonly referred to as catalyst-transfer polymerization (CTP).⁴³ This methodology is especially useful for the synthesis of π -conjugated polymers with narrow polydispersity. The key difference between step-growth polymerization and CTP is ring-walking, wherein the catalyst remains bound to the π -system (**9**) before migrating to the next C-X terminus.⁴⁴ After migration, intramolecular oxidative addition at the C-X bond then repeats the catalytic cycle. This cycle continues until all C-X sites have been coupled. The ring-walking behavior of CTP systems has also been supported by both experimental and computational data.⁴⁵

Creating a mechanistic model in COPASI using the reaction network in Scheme 4, which invokes **9** as a key intermediate, allows the formation of reaction profiles not possible using the previous linear pathway (Figure 8). Accounting for the equilibrium process between **6** and **9** resulted in the closest fits yet to match the trends associated with **6** and **8** (Figure 8b). This updated model better recapitulates the observed profiles but does not accurately match the zero order profiles of each species. To more accurately model the observed reaction profile, additional mechanistic inferences must be included in the model, such as off-cycle equilibria or product effects.

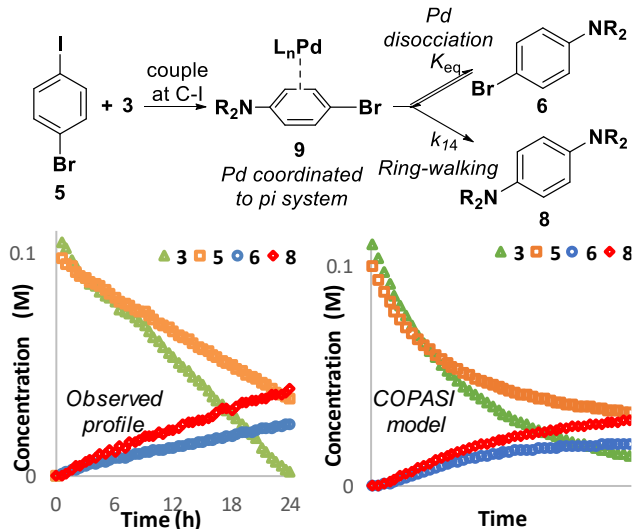


Figure 8. Comparing observed kinetic data with a COPASI model for the coupling cascade reaction using **5**. a) Reaction profile described in Figure 6. b) COPASI model generated using reaction network in Scheme 4.

Considering whether the linear reaction network in Figure 7 or the catalyst transfer process (CTP) in Figure 8 best describes the cascade reaction with substrate **5**, we believe the CTP pathway is occurring. The combination of a better COPASI product distribution and literature precedence lead us to this conclusion. To the best of our knowledge, this catalyst-transfer type behavior has not been reported in Buchwald-Hartwig aminations, or for any coupling reaction using a heteroatom.

CONCLUSION

We have developed a modular reaction monitoring platform capable of automated sampling from reactions performed within a glovebox and coupled it with online HPLC analysis. The ability of the platform to dilute, deliver, and analyze reaction aliquots was demonstrated to be highly reproducible by trending the response when a vial of toluene was sampled from within a glovebox and analyzed 50 times. We also observed a characteristic relationship between diluent volume and detector response which allows for a wide range of reaction concentrations to be monitored. We used the sampling platform to generate reaction profiles for a series of Buchwald-Hartwig aminations. Reactions with aryl halides iodobenzene and bromobenzene performed in parallel demonstrate distinct profiles, neither of which displayed classical kinetics. A competition reaction using both aryl halides displayed unexpected catalyst monopoly by coupling iodobenzene over bromobenzene when both were present in similar concentrations. An additional unanticipated reaction profile was observed when the dihalogenated substrate 1-bromo-4-iodobenzene was employed. The temporal profiles of each component displayed 0 order kinetics. Additionally, the product after two sequential aminations was observed at the first data point demonstrating the formation of the dicoupled product is facile. We invoke ring-walking behavior of the Pd catalyst in this system to rationalize the observed trends. To the best of our knowledge this is the first example of ring walking behavior in coupling reactions involving heteroatoms.

AUTHOR INFORMATION

Corresponding Author

jhein@chem.ubc.ca

Notes

The authors declare no competing financial interests.

ACKNOWLEDGMENTS

The authors gratefully acknowledge Mettler-Toledo Autochem for generous donation of process analytical equipment (ReactIR and EasyMax). Financial support for this work was provided by the University of British Columbia, the Canadian Foundation for Innovation (CFI-35883), and the Natural Sciences and Engineering Research Council of Canada (RCPIN-2016-04613, CRDPJ 530118-18). Student support was provided by an NSERC CGSD scholarship (TCM).

REFERENCES

- (1) Malig, T. C.; Koenig, J. D. B.; Situ, H.; Chehal, N. K.; Hultin, P. G.; Hein, J. E. Real-Time HPLC-MS Reaction Progress

- Monitoring Using an Automated Analytical Platform. *React. Chem. Eng.* **2017**, *2* (3), 309–314.
- (2) Malig, T. C.; Yu, D.; Hein, J. E. A Revised Mechanism for the Kinugasa Reaction. *J. Am. Chem. Soc.* **2018**, *140* (29), 9167–9173.
 - (3) Dorel, R.; Grugel, C. P.; Haydl, A. M. The Buchwald-Hartwig Amination After 25 Years. *Angew. Chem. Int. Ed.* **2019**, *58* (48), 17118–17129.
 - (4) Hartwig, J. F. Transition Metal Catalyzed Synthesis of Arylamines and Aryl Ethers from Aryl Halides and Triflates: Scope and Mechanism. *Angew. Chem. Int. Ed.* **1998**, *37* (15), 2046–2067.
 - (5) Yang, B. H.; Buchwald, S. L. Palladium-Catalyzed Amination of Aryl Halides and Sulfonates. *J. Organomet. Chem.* **1999**, *576* (1–2), 125–146.
 - (6) Heravi, M. M.; Kheilkordi, Z.; Zadsirjan, V.; Heydari, M.; Malmir, M. Buchwald-Hartwig Reaction: An Overview. *J. Organomet. Chem.* **2018**, *861*, 17–104.
 - (7) Guram, A. S.; Buchwald, S. L. Palladium-Catalyzed Aromatic Aminations with in Situ Generated Aminostannanes. *J. Am. Chem. Soc.* **1994**, *116* (17), 7901–7902.
 - (8) Paul, F.; Patt, J.; Hartwig, J. F. Palladium-Catalyzed Formation of Carbon-Nitrogen Bonds. Reaction Intermediates and Catalyst Improvements in the Hetero Cross-Coupling of Aryl Halides and Tin Amides. *J. Am. Chem. Soc.* **1994**, *116* (13), 5969–5970.
 - (9) Tasler, S.; Mies, J.; Lang, M. Applicability Aspects of Transition Metal-Catalyzed Aromatic Amination Protocols in Medicinal Chemistry. *Adv. Synth. Catal.* **2007**, *349* (14–15), 2286–2300.
 - (10) Cooper, T. W. J.; Campbell, I. B.; Macdonald, S. J. F. Factors Determining the Selection of Organic Reactions by Medicinal Chemists and the Use of These Reactions in Arrays (Small Focused Libraries). *Angew. Chem. Int. Ed.* **2010**, *49* (44), 8082–8091.
 - (11) Roughley, S. D.; Jordan, A. M. The Medicinal Chemist's Toolbox: An Analysis of Reactions Used in the Pursuit of Drug Candidates. *J. Med. Chem.* **2011**, *54* (10), 3451–3479.
 - (12) Surry, D. S.; Buchwald, S. L. Biaryl Phosphane Ligands in Palladium-Catalyzed Amination. *Angew. Chem. Int. Ed.* **2008**, *47* (34), 6338–6361.
 - (13) Blaser, H. U.; Indolese, A.; Naud, F.; Nettekoven, U.; Schnyder, A. Industrial R&D on Catalytic C-C and C-N Coupling Reactions: A Personal Account on Goals, Approaches and Results. *Adv. Synth. Catal.* **2004**, *346* (13–15), 1583–1598.
 - (14) Mari, M.; Bartocchini, F.; Piersanti, G. Synthesis of (-)-Epi-Indolactam v by an Intramolecular Buchwald-Hartwig C-N Coupling Cyclization Reaction. *J. Org. Chem.* **2013**, *78* (15), 7727–7734.
 - (15) Foo, K.; Newhouse, T.; Mori, I.; Takayama, H.; Baran, P. S. Total Synthesis Guided Structure Elucidation of (+)-Psychotramine. *Angew. Chem. Int. Ed.* **2011**, *50* (12), 2716–2719.
 - (16) Nozaki, K.; Takahashi, K.; Nakano, K.; Hiyama, T.; Tang, H.-Z.; Fujiki, M.; Yamaguchi, S.; Tamao, K. The Double N-Arylation of Primary Amines: Toward Multisubstituted Carbazoles with Unique Optical Properties. *Angew. Chem. Int. Ed.* **2003**, *42* (18), 2051–2053.
 - (17) Devendar, P.; Qu, R. Y.; Kang, W. M.; He, B.; Yang, G. F. Palladium-Catalyzed Cross-Coupling Reactions: A Powerful Tool for the Synthesis of Agrochemicals. *J. Agric. Food Chem.* **2018**, *66* (34), 8914–8934.
 - (18) Widenhoefer, R. A.; Zhong, H. A.; Buchwald, S. L. Synthesis and Solution Structure of Palladium Tris(o-Tolyl)Phosphine Mono(Amine) Complexes. *Organometallics* **1996**, *15* (12), 2745–2754.
 - (19) Widenhoefer, R. A.; Buchwald, S. L. Formation of Palladium Bis(Amine) Complexes from Reaction of Amine with Palladium Tris(o-Tolyl)Phosphine Mono(Amine) Complexes. *Organometallics* **1996**, *15* (16), 3534–3542.
 - (20) Chung, R.; Hein, J. E. Automated Solubility and Crystallization Analysis of Non-UV Active Compounds: Integration of Evaporative Light Scattering Detection (ELSD) and Robotic Sampling. *React. Chem. Eng.* **2019**, *4* (9), 1674–1681.
 - (21) Daponte, J. A.; Guo, Y.; Ruck, R. T.; Hein, J. E. Using an Automated Monitoring Platform for Investigations of Biphasic Reactions. *ACS Catal.* **2019**, *9* (12), 11484–11491.
 - (22) Rougeot, C.; Situ, H.; Cao, B. H.; Vlachos, V.; Hein, J. E. Automated Reaction Progress Monitoring of Heterogeneous Reactions: Crystallization-Induced Stereoselectivity in Amine-Catalyzed Aldol Reactions. *React. Chem. Eng.* **2017**, *2* (2), 226–231.
 - (23) Fitton, P.; Rick, E. A. The Addition of Aryl Halides to Tetrakis(Triphenylphosphine)Palladium(0). *J. Organomet. Chem.* **1971**, *28* (2), 287–291.
 - (24) Barrios-Landeros, F.; Carrow, B. P.; Hartwig, J. F. Effect of Ligand Steric Properties and Halide Identity on the Mechanism for Oxidative Addition of Haloarenes to Trialkylphosphine Pd(0) Complexes. *J. Am. Chem. Soc.* **2009**, *131* (23), 8141–8154.
 - (25) Barrios-Landeros, F.; Hartwig, J. F. Distinct Mechanisms for the Oxidative Addition of Chloro-, Bromo-, and Iodoarenes to a Bisphosphine Palladium(0) Complex with Hindered Ligands. *J. Am. Chem. Soc.* **2005**, *127* (19), 6944–6945.
 - (26) Espinet, P.; Echavarren, A. M. The Mechanisms of the Stille Reaction. *Angewandte Chem. International Edition*. John Wiley & Sons, Ltd September 13, 2004, pp 4704–4734.
 - (27) Arrechea, P. L.; Buchwald, S. L. Biaryl Phosphine Based Pd(II) Amido Complexes: The Effect of Ligand Structure on Reductive Elimination. *J. Am. Chem. Soc.* **2016**, *138* (38), 12486–12493.
 - (28) Shekhar, S.; Ryberg, P.; Hartwig, J. F.; Mathew, J. S.; Blackmond, D. G.; Strieter, E. R.; Buchwald, S. L. Reevaluation of the Mechanism of the Amination of Aryl Halides Catalyzed by BINAP-Ligated Palladium Complexes. *J. Am. Chem. Soc.* **2006**, *128* (11), 3584–3591.
 - (29) Senn, H. M.; Ziegler, T. Oxidative Addition of Aryl Halides to Palladium(0) Complexes: A Density-Functional Study Including Solvation. *Organometallics* **2004**, *23* (12), 2980–2988.
 - (30) Blanksby, S. J.; Ellison, G. B. Bond Dissociation Energies of Organic Molecules. *Acc. Chem. Res.* **2003**, *36* (4), 255–263.
 - (31) Surry, D. S.; Buchwald, S. L. Dialkylbiaryl Phosphines in Pd-Catalyzed Amination: A User's Guide. *Chem. Sci.* **2011**, *2* (1), 27–50.
 - (32) Fors, B. P.; Krattiger, P.; Strieter, E.; Buchwald, S. L. Water-Mediated Catalyst Preactivation: An Efficient Protocol for

C-N Cross-Coupling Reactions. *Org. Lett.* **2008**, *10* (16), 3505–3508.

- (33) Hartwig, J. F.; Kawatsura, M.; Hauck, S. I.; Shaughnessy, K. H.; Alcazar-Roman, L. M. Room-Temperature Palladium-Catalyzed Amination of Aryl Bromides and Chlorides and Extended Scope of Aromatic C-N Bond Formation with a Commercial Ligand. *J. Org. Chem.* **1999**, *64* (15), 5575–5580.
- (34) Yamamoto, T.; Nishiyama, M.; Koie, Y. Palladium-Catalyzed Synthesis of Triarylamines from Aryl Halides and Diarylamines. *Tetrahedron Lett.* **1998**, *39* (16), 2367–2370.
- (35) Guram, A. S.; Rennels, R. A.; Buchwald, S. L. A Simple Catalytic Method for the Conversion of Aryl Bromides to Arylamines. *Angew. Chem. Int. Ed.* **1995**, *34* (12), 1348–1350.
- (36) Louie, J.; Hartwig, J. F. Palladium-Catalyzed Synthesis of Arylamines from Aryl Halides. Mechanistic Studies Lead to Coupling in the Absence of Tin Reagents. *Tetrahedron Lett.* **1995**, *36* (21), 3609–3612.
- (37) Sadighi, J. P.; Harris, M. C.; Buchwald, S. L. A Highly Active Palladium Catalyst System for the Arylation of Anilines. *Tetrahedron Lett.* **1998**, *39* (30), 5327–5330.
- (38) Meyers, C.; Maes, B. U. W.; Loones, K. T. J.; Bal, G.; Lemièrre, G. L. F.; Dommissie, R. A. Study of a New Rate Increasing “Base Effect” in the Palladium-Catalyzed Amination of Aryl Iodides. *J. Org. Chem.* **2004**, *69* (18), 6010–6017.
- (39) Ferretti, A. C.; Mathew, J. S.; Ashworth, I.; Purdy, M.; Brennan, C.; Blackmond, D. G. Mechanistic Inferences Derived from Competitive Catalytic Reactions: Pd(Binap)-Catalyzed Amination of Aryl Halides. *Adv. Synth. Catal.* **2008**, *350* (7–8), 1007–1012.
- (40) Newman, S. G.; Lautens, M. The Role of Reversible Oxidative Addition in Selective Palladium(0)-Catalyzed Intramolecular Cross-Couplings of Polyhalogenated Substrates: Synthesis of Brominated Indoles. *J. Am. Chem. Soc.* **2010**, *132* (33), 11416–11417.
- (41) Roy, A. H.; Hartwig, J. F. Directly Observed Reductive Elimination of Aryl Halides from Monomeric Arylpalladium(II) Halide Complexes. *J. Am. Chem. Soc.* **2003**, *125* (46), 13944–13945.
- (42) Roy, A. H.; Hartwig, J. F. Reductive Elimination of Aryl Halides from Palladium(II). *J. Am. Chem. Soc.* **2001**, *123* (6), 1232–1233.
- (43) Leone, A. K.; Mueller, E. A.; McNeil, A. J. The History of Palladium-Catalyzed Cross-Couplings Should Inspire the Future of Catalyst-Transfer Polymerization. *J. Am. Chem. Soc.* **2018**, *140* (45), 15126–15139.
- (44) Leone, A. K.; Goldberg, P. K.; McNeil, A. J. Ring-Walking in Catalyst-Transfer Polymerization. *J. Am. Chem. Soc.* **2018**, *140* (25), 7846–7850.
- (45) Mikami, K.; Nojima, M.; Masumoto, Y.; Mizukoshi, Y.; Takita, R.; Yokozawa, T.; Uchiyama, M. Catalyst-Dependent Intrinsic Ring-Walking Behavior on π -Face of Conjugated Polymers. *Polym. Chem.* **2017**, *8* (10), 1708–1713.
-